Research Article

Fernblock® Upregulates NRF2 Antioxidant Pathway and Protects Keratinocytes from PM$_{2.5}$-Induced Xenotoxic Stress

Pablo Delgado-Wicke [ID],[1] **Azahara Rodríguez-Luna** [ID],[2] **Yoshifumi Ikeyama** [ID],[3] **Yoichi Honma,**[3] **Toshiaki Kume,**[4] **María Gutierrez** [ID],[1] **Silvia Lorrio,**[1] **Ángeles Juarranz** [ID],[1,5] **and Salvador González** [ID][5,6]

[1]*Department of Biology, Faculty of Sciences, Autónoma University of Madrid (UAM) 28049, Madrid, Spain*
[2]*Medical Affairs Department, Cantabria Labs, 28043 Madrid, Spain*
[3]*Rohto Basic Research Development Division, Tokyo, Japan*
[4]*Department of Applied Pharmacology, Graduate School of Medicine and Pharmaceutical Sciences, University of Toyama, Sugitani, Toyama, Japan*
[5]*Instituto Ramón y Cajal de Investigación Sanitaria (IRYCIS), Madrid, Spain*
[6]*Department of Medicine and Medical Specialties, Alcalá de Henares University, 28805 Madrid, Spain*

Correspondence should be addressed to Ángeles Juarranz; angeles.juarranz@uam.es
and Salvador González; salvagonrod@gmail.com

Pablo Delgado-Wicke and Azahara Rodríguez-Luna contributed equally to this work.

Humans in modern industrial and postindustrial societies face sustained challenges from environmental pollutants, which can trigger tissue damage from xenotoxic stress through different mechanisms. Thus, the identification and characterization of compounds capable of conferring antioxidant effects and protection against these xenotoxins are warranted. Here, we report that the natural extract of *Polypodium leucotomos* named Fernblock®, known to reduce aging and oxidative stress induced by solar radiations, upregulates the NRF2 transcription factor and its downstream antioxidant targets, and this correlates with its ability to reduce inflammation, melanogenesis, and general cell damage in cultured keratinocytes upon exposure to an experimental model of fine pollutant particles (PM$_{2.5}$). Our results provide evidence for a specific molecular mechanism underpinning the protective activity of Fernblock® against environmental pollutants and potentially other sources of oxidative stress and damage-induced aging.

1. Introduction

Air pollution is a growing challenge to public health worldwide and constitutes an emerging focus of research and surveillance for the World Health Organization [1]. Because of the role of the skin as a primary barrier against external sources of tissue damage, continuous exposure to these pollutants has a substantial negative impact on this organ and is precursor of premature skin aging, pigmentation, acne disorders, and psoriasis exacerbation, among others [2]. Specifically, PM$_{2.5}$ provokes increased ROS and loss of organelle homeostasis in keratinocytes [3], has been associated with aggravated allergic dermatitis and eczema in children [4], and is precursory to inflammation, aging, androgenic alopecia, and skin cancer [5]. Thus, air pollution, solar radiation, and tobacco smoke constitute extrinsic skin-aging factors, leading to ROS production and the subsequent activation of oxidative stress responses. Skin antioxidant defense responses are effective against these exogenous sources of damage; however, chronic exposure, aging, or several

concomitant pathologies can lead to decreased activation and increased oxidative damage, accelerating skin aging and skin cancer [6]. Prevention strategies including sun protection, skin barrier improvement, aryl hydrocarbon receptor (AhR) modulation [7], and increased skin tissue resistance through potentiation of natural detoxification pathways are target opportunities for skin protection [8]. Fully understanding mechanisms by which tissues confront these sources of xenotoxic stress and potential pharmacological opportunities to leverage on them are warranted.

Nuclear factor erythroid 2-related factor 2 (NRF2; also known as nuclear factor erythroid-derived 2-like 2, NFE2L2) is a basic leucine zipper transcription factor highly conserved in metazoans [9]. In nonstressed cells, the NRF2 protein is bound in the cytoplasm, ubiquitinated and rapidly degraded to low levels by the Kelch-like ECH-associated protein 1- (KEAP1-) Cullin 3 ubiquitin ligase complex. Generic insults provoking oxidative or electrophilic stress in cells inactivate the KEAP1/CUL3 complex, promoting nuclear translocation of accumulating NRF2, which in turn orchestrates the expression of different antioxidant enzymes (including most components of the glutathione de novo synthesis pathway and glutathione transferases and peroxidases) and detoxifying effectors (NAD(P)H Quinone Dehydrogenase 1 (NQO1), heme oxygenase 1 (HO-1), or Multidrug Resistant Proteins (MRPs)) in most cell types [10]. NRF2 constitutes an emerging, appealing target for therapeutic modulation in multiple pathologies [11]. Of note, NRF2 activity has been specifically associated with response to various environmental pollutants that potentially act as xenotoxins, including air $PM_{2.5}$ [12, 13].

Fernblock® is a natural standardized aqueous extract from the leaves of *Polypodium leucotomos* [14]. The use of decoctions of this fern was widespread in traditional medicine amongst local indigenous populations in Central America against numerous ailments, and modern medicine has confirmed its notable potential as an active conferring skin-specific antioxidant activity and protection against sun radiation damage (including aging, hyperpigmentation, and DNA damage) [15]. However, while evidence supporting a boosting of endogenous antioxidant and xenobiotic stress systems in cells is highly relevant for the therapeutic potential of Fernblock® [16–18], our understanding of the molecular mechanisms by which this occurs is limited.

Here, we contribute evidence suggesting that Fernblock® is capable of upregulating the NRF2 pathway as assessed by different direct and indirect readouts in cultured human cells and that this dose-dependent activation correlates with its protective effect not only against UVB radiation but also against exposure to $PM_{2.5}$. These observations suggest a potential for Fernblock® not only as a natural activity against the detrimental effects of a broad range of environmental sources of xenobiotic stress and aging but also as a potential tool for activating the NRF2 pathway.

2. Materials and Methods

2.1. Cell Culture and Treatments.
The nontumorigenic human keratinocyte cell line HaCaT was used for *in vitro* studies (Cell Line Service, Eppelheim, Germany). Cells were subcultured in different plate formats according to assay (see below), in Dulbecco's modified Eagle's medium (DMEM) supplemented with 10% (v/v) fetal bovine serum (FBS), 50 units/ml penicillin, and 50 μg/ml streptomycin, in an incubator at 5% CO_2, 37°C, and 95% humidity. Rat adrenal pheochromocytoma PC12 cells were maintained in Dulbecco's modified Eagle's medium supplemented with 5% fetal calf serum and 10% horse serum. All cell culture reagents were purchased from Gibco Inc. (Paisley, UK). Human Epidermal Keratinocytes (NHEK; KURABO Co., Japan; Cat. No. KM4109, Lot No. 04644) were grown in HuMedia KG2 (KURABO Cat. No. KK-2150S) and assayed in HuMedia KB2 (KURABO Cat. No. KK-2350S). Human vaginal malignant melanoma cells (HMVII; European Collection of Authenticated Cell Cultures (ECACC), UK; Cat. No. 92042701, Lot No. 14B033) were grown and assayed in RPMI1640, supplemented with 10% FBS and penicillin-streptomycin. All cell culture reagents were purchased from Gibco Inc. (Paisley, UK).

Treatments as described in different experiments were applied on cultures at 50-60% confluence from 10 mg/ml stocks in all cases, and FBS supplementation was reduced to 1%. Fernblock® was provided by Cantabria Labs (Spain). A Standard Reference Material (SRM) for experimental modelling of air pollutants at $PM_{2.5}$ was purchased from Sigma-Aldrich (UK; Diesel Particulate Matter 1650b) and was routinely sonicated to avoid aggregation for 30 min′ for immediate use during the next hour. Sulforaphane was purchased from Sigma-Aldrich (Japan; Sulforaphane S4441-5MG).

2.2. Reagents and Antibodies.
Cell viability was measured using an assay based on MTT (3-(4,5-dimethylthiazol-2-yl)-2,5-diphenyltetrazolium bromide) (Sigma-Aldrich, St Louis, USA). The following primary antibodies were used in the performed immunofluorescence and western blot assays: mouse anti α-tubulin (Sigma-Aldrich, St Louis, USA), anti-beclin1 (Cell Signaling, #3738), anti-HO-1 (Cell Signaling, #70081), anti-LC3 (Abcam, Ab58610), anti-NQO1 (Cell Signaling, #3187), and anti-NRF2 (Abcam, ab89443), The secondary antibodies employed were mouse IgG-Alexa 488 and rabbit IgG-Alexa 546 (Invitrogen, Oregon, USA) and mouse IgG peroxidase and rabbit IgG peroxidase (Thermo Scientific, Rockford, USA). The markers used for the *in vivo* staining were monodansylcadaverine (MDC) for phagolysosomes and LysoTracker Green (LTG) for lysosomes. Hoechst 33258 (Sigma-Aldrich) was used for cellular staining.

2.3. Luciferase Assays for NRF2 Activity in PC12 Cells.
Complementary oligonucleotides spanning a functional antioxidant response element (ARE) from the human NQO1 gene reference promoter sequence (-473 to -440) were annealed and ligated into the pGL4.27 vector (Promega, Madison, WI, USA). The resulting reporter vector was stably transfected onto PC12 using Lipofectamine 2000 (Invitrogen, Carlsbad, CA, USA) according to the manufacturer's instructions. Firefly activity in cell lysates from each assayed condition was measured in a luminometer using a Picagene LT2.0 Luminescence Reagent (Toyo Ink, Tokyo, Japan) according to the manufacturer's instructions. Results shown are derived

as mean values and standard deviations from three independent experiments.

2.4. Assays for Studying UVB-Induced Damage in Human Keratinocytes. NHEKs were seeded onto 6-well culture plates at 300,000 cells/well. After 24 h spreading, cells were switched to KB2 medium supplemented with either vehicle (DMSO) or 31.3 μg/ml Fernblock® for 24 additional hours. Cultures were then rinsed in PBS, irradiated with UVB (90 mJ/cm^2) using a F1215 unit (Muranaka Medical Instruments Co. Ltd., Japan), and further cultured in KB2 for 6 h (cytokine expression assays), 24 h (cell counting and NRF2 activity assays), or 72 h (melanization assays).

Cell counting was automated from Hoechst 33342-stained samples using the ImageXpress Micro platform (Molecular Devices LLC, San José, CA, USA). For gene expression assays, total cell RNA was isolated using the RNeasy mini kits (QIAGEN) and reverse-transcribed using ReverTra Ace technology (Toyobo Co., Osaka, Japan). cDNAs were then quantitated by real-time PCR $^{(-\Delta\Delta Ct}$ method) using the ABI TaqMan™ Fast Advanced Master Mix (Thermo Scientific, USA) and the following ABI TaqMan™ probes for human sequences: catalase (CAT) (Hs00156308_m1), glutathione peroxidase (GPX) (ABI TaqMan Probe: Hs00829989_gH), GPX 4 (ABI TaqMan Probe: Hs00157812_m1), HO-1 (ABI TaqMan Probe: Hs00157 965_m1), NQO1 (ABI TaqMan Probe: Hs00168547_m1), interleukin (IL)6 (ABI TaqMan Probe: Hs00174131_m1), and IL8 (ABI TaqMan Probe: Hs00174103_m1).

Melanin production was assayed as follows: KB2 72 h-conditioned medium from NHEKs supplemented and irradiated as indicated (see above) was diluted 1 : 1 with HMVII medium and added to a monolayer of HMVII cells 24 h post-seeding. After 48 h culture for uptake, HMVII cells were trypsinized, pelleted, and treated with 2 N NaOH for 40 min at 80°C. Melanin content was measured by absorbance within a 405 nm–620 nm range using a plate spectrophotometer, corrected for cell viability (as assessed by trypan blue exclusion staining), and normalized to values observed in cells exposed to supernatants from nonirradiated cells ("control").

2.5. Cellular Toxicity in PM$_{2.5}$-Exposed HaCaT Keratinocytes. Toxicity of different concentrations of Fernblock® and PM$_{2.5}$was inferred by the MTT colorimetric assay in HaCaT cells 24 and 48 h posttreatment. Briefly, cells were exposed after indicated treatment times to 50 μg/ml MTT (3-(4,5-dimethyl-thiazol-2-yl)-2,5-diphenyltetrazolium bromide) at 37°C for 3 hours in the dark. Precipitated formazan was solubilized in DMSO (PanReac, Barcelona, Spain), and absorption was measured at 542 nm in a spectrophotometer (Spectra Fluor, Tecan). Cellular toxicity was expressed as the percentage of formazan absorption from the different treatment conditions compared to nontreated cells. Results shown are derived as mean values and standard deviations from three independent experiments.

2.6. Immunofluorescence Microscopy and Image Analysis. Active formation of phagolysosomal vacuoles was monitored by incubation of cells grown on coverslips with MDC for 10 min. Lysosomal compartment was decorated with Lyso-Tracker Green™ (Molecular Probes), following the manufacturer's instructions. After briefly washing cells with PBS, slides were immediately mounted for image acquisition under UV or green excitation light.

For immunostaining, cells grown on the coverslips were fixed in a 3.7% formaldehyde solution in PBS for 10 min, washed with PBS 1X three times, and permeabilized with Triton X-100 0.1% in PBS during 30 min in agitation. Samples were incubated with primary antibodies for 1 h at 37°C, inside a humid chamber. After washing with PBS, cells were incubated with secondary antibodies for 45 min at 37°C. Nuclei were counterstained with Hoechst 33258. Coverslips were then washed with PBS and mounted with ProLong® antifade mounting medium (Molecular Probes). Images were acquired on an Olympus BX61 epifluorescence microscope equipped with filter sets for fluorescence microscopy: ultraviolet (exciting filter BP360-390), blue (exciting filter BP460-490), and green (exciting filter BP510-550), coupled to an Olympus CCD DP70 digital camera. LC3 immunofluorescence was quantified using ImageJ from at least fifty cells from each condition. NRF2 activation was assessed by separately computing nuclear and cytoplasmic intensities, from fifty cells from each condition. Figures were prepared using the Adobe Photoshop CS5 extended version 12.0 software (Adobe Systems Inc., USA).

2.7. Western Blotting. Cells were lysed in RIPA buffer (150 mM NaCl, 1% Triton X-100, 1% deoxycholate, 0.1% SDS, 10 mM Tris-HCl pH 7.2, and 5 mM EDTA), supplemented with phosphatase inhibitors and protease inhibitor cocktail tablets (Sigma-Aldrich, St. Louis, MO). Protein concentration was measured by BCA assay (Thermo Scientific-Pierce, Rockford, USA). Protein samples were subjected to SDS-PAGE and blotted to Immobilon-P PVDF membranes (Millipore Co., Massachusetts, USA). Membranes were blocked in PBS-tween 0.1% with 5% nonfat dried milk for 1 h at 25°C and then incubated with primary antibodies overnight at 4°C. After extensive washing with PBS-tween 0.1%, membranes were incubated with peroxidase-conjugated secondary antibodies. Signal was developed by chemiluminescence (ECL, Amersham Pharmacia Biotech, Little Chalfont, UK) and acquired on a ChemiDocTR XRS+ high definition system (Bio-Rad). Bands corresponding to the different proteins were digitalized employing the Image Lab version 3.0.1 (Bio-Rad Laboratories). This assay was performed at least three times for each target.

2.8. Statistical Analysis. Data are expressed as the mean value of at least three experiments ± standard deviations (SD). The statistical analysis was made using the statistical package of the program GraphPad Prism 6. Statistical significance was determined using a *t*-test and analysis of variance (ANOVA), and $p < 0.05$ was considered statistically significant.

3. Results

3.1. Fernblock® Induces a NRF2-Dependent Transcriptional Pathway which Correlates with Its Protection against UVB Radiation. Previous studies demonstrated that Fernblock®

is capable of exerting a protective effect on cells against UVB irradiation [15–19]. Thus, we first corroborated that Fernblock® treatment had no toxic effect against cell viability (Figure 1(a)), as well as its protective effect attenuating UVB-induced decrease in cell proliferation/viability, as assessed by normalized cell count (Figure 1(b)). However, the molecular mechanisms by which this occurs are not completely characterized. We decided to test the ability of Fernblock® to induce a major endogenous pathway deployed by cells to counteract oxidative and electrophilic stress: the NRF2 pathway.

First, we employed an established cell line of ectodermal lineage (PC12 pheochromocytoma cell line, widely used as a model for studying NRF2 activity [20]), stably expressing a luciferase reporter under the control of a promoter fragment derived from the canonical NRF2 target NAD(P)H Quinone Dehydrogenase 1 (NQO1). Several studies report that the exposure to the organosulfur compound sulforaphane leads to increased transcription of nuclear NRF2 and downstream cytoprotective genes [20–22]. Of note, Fernblock® induced the reporter in a concentration-dependent manner, suggesting that it is capable of upregulating this protective pathway in cells (Figure 1(c)).

We then investigated whether this effect also occurs in keratinocytes and whether it is associated with specific protection from exposure to UVB radiation. qRT-PCR assessment of mRNA levels for several bona fide targets of NRF2 (CAT, GPX 1 and 4, HO-1, and NQO1) revealed that Fernblock® induces the transcription of all these genes in human keratinocytes in a concentration-dependent manner (Figures 1(d)–1(h)). Similar antioxidant effects have been previously observed in a different *in vitro* model with a sulforaphane combination.

Importantly, in line with previous results, these treatment routines with Fernblock® protected keratinocytes from UVB radiation, decreased UVB-dependent induction of inflammatory cytokines IL6 and IL8 (Figure 1(i)), and significantly reduced the induction of melanin production (Figure 1(j)). Because NRF2 is a well-established prosurvival and anti-inflammatory pathway [10, 11], we consider the association of NRF2 induction with protection from UVB-induced damage in cells exposed to Fernblock® to be functionally relevant.

3.2. Fernblock® Protects Human Keratinocytes from Damage Induced by Fine Particle Pollutants (PM$_{2.5}$) in an In Vitro Model. The protective effect of Fernblock® against a broad spectrum of solar radiation is well established [16–18]. We considered whether this protective mechanism might also operate in a different condition leading to severe cell stress: high exposure to fine particle pollutants (PM$_{2.5}$). Exposure of keratinocytes to a SRM of PM$_{2.5}$ decreased cell viability in a concentration-dependent manner (Figure 2). On the other hand, simultaneous addition of Fernblock® in concentrations previously shown to induce NRF2 and protect from UVB-induced cell damage partially reverted toxicity associated with low to moderate concentrations of PM$_{2.5}$ (25-50 μg/ml; Figure 2), although higher PM$_{2.5}$ doses were not counteracted in this *in vitro* model (Figure 2). The selected

PM$_{2.5}$ dose was 50 μg/ml for all experiments. Fernblock® doses did not have any intrinsic effect on cell viability in the absence of PM$_{2.5}$ (Figures 1(a) and 2).

3.3. Fernblock® Increases Basal and PM$_{2.5}$-Induced Autophagy in Keratinocytes. We assessed the formation of autophagolysosomal vacuoles to infer canonical autophagy activation, indicative of cell adaption to generic stress. We first visualised the formation of autophagolysosomal vacuoles by MDC staining, as well as expansion of the lysosomal compartment as decorated by LysoTracker Green™. Consistent with a robust induction of xenotoxic stress, visual inspection revealed that exposure to PM$_{2.5}$ increased the formation of autophagolysosomes (MDC+-positive mask) and was associated with an enlargement of the lysosomal compartment (LysoTracker Green+ mask) (Figure 3(a) second column of panels from left), both established features of prosurvival cell adaptive responses. Addition of Fernblock® further enhanced this expansion of the phagolysosomal compartment, and Fernblock® addition alone was also associated with a mild increase in the MDC/LysoTracker+ area (Figure 3(a), right panel columns). These observations are in agreement with experiments assessing relative density of LC3 puncta (indicative of *de novo* phagosome formation and maturation and activation of autophagy flux): Fernblock® increases basal autophagy flux in healthy cells and further enhances the activation provoked by PM$_{2.5}$ exposure, consistent with its protective effect (Figures 3(b) and 3(c)).

These observations suggest that Fernblock® promotes the activation of survival pathways naturally employed by cells in the face of homeostasis challenges, and this induction correlates with its prosurvival and protective effects.

3.4. Fernblock® Upregulates NRF2 Basal Activity and Increases NRF2 Induction upon Exposure to PM$_{2.5}$. Because NRF2 activity is reported to be sensitive to xenotoxic stress from air pollutants [12, 13, 23], and our preliminary data demonstrated that the NRF2-dependent transcriptional pathway is triggered by treatment with Fernblock® (Figure 1), we moved to determine the relationship between Fernblock®-induced protection against PM$_{2.5}$ toxicity and NRF2 regulation. Immunostaining revealed that unchallenged HaCaT keratinocytes in culture have low total and nuclear levels of NRF2 protein (Figures 4(a) and 4(b)). In accordance with the activation of an adaptive cytoprotective response, PM$_{2.5}$ exposure alone leads to a robust increase in total NRF2 levels. Of note, Fernblock® exposure led *per se* to a mild increase specifically of NRF2 nuclear pools and further boosted NRF2 levels in cells exposed to PM$_{2.5}$ (Figures 4(a) and 4(b)). Of note, Fernblock® did not entail the acute increase in cytoplasmic pools of NRF2 observed in cells exposed to PM$_{2.5}$ (fig. S1, see Figure 4(a)).

We further assessed activation of the pathway downstream NRF2 by assessing the levels of two bona fide transcriptional targets of NRF2: NQO1 and HO-1. In line with our previous observations for NRF2 protein levels, PM$_{2.5}$ exposure markedly upregulated NQO1 protein levels as assessed by immunofluorescent staining and western blot in HaCaT cells (Figures 4(c) and 4(d)). Fernblock® promoted
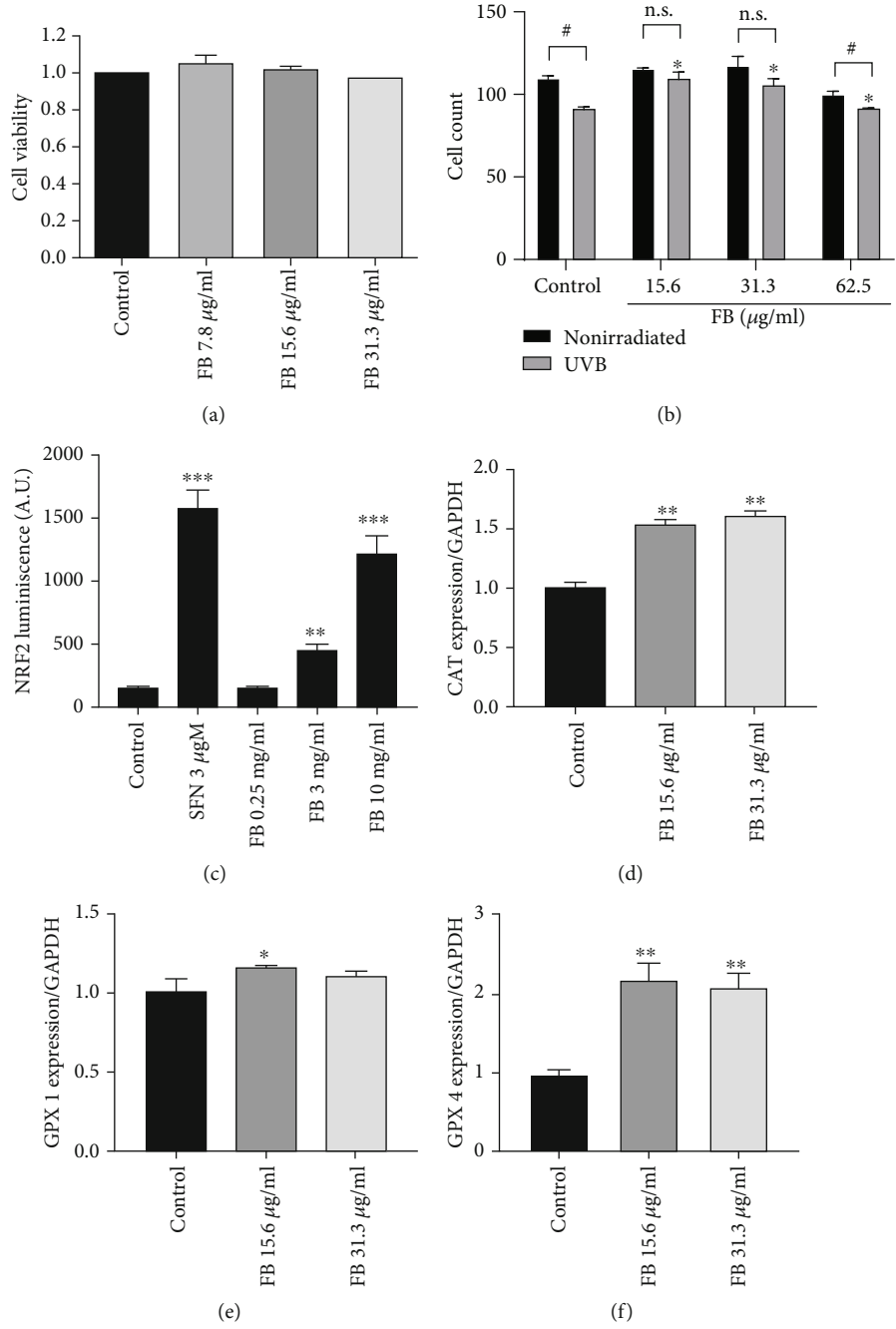
(a)

(b)

(c)

(d)

(e)

(f)

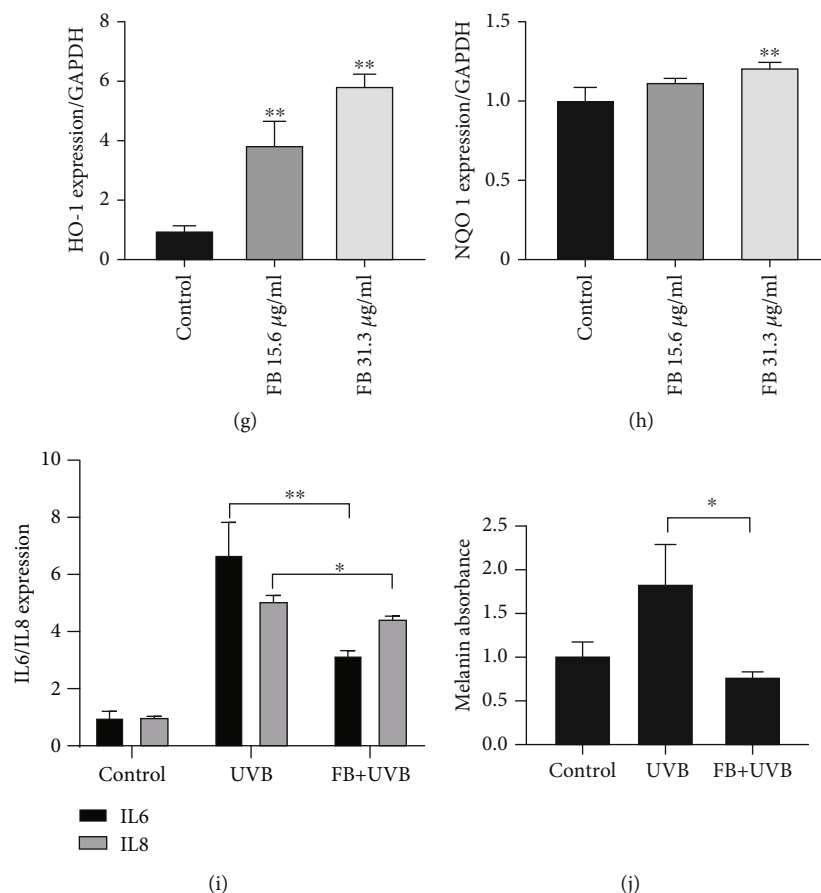Figure 1: Continued.

(g)

(h)

(i)

(j)

FIGURE 1: Fernblock® (FB) induces NRF2-dependent transcription activity and attenuates UVB-induced inflammation and melanization. (a) Fernblock® supplementation does not have a significant impact on cell viability as assessed by MTT assay. Data derived from 3 independent replicates and normalized to vehicle-treated samples (black bar, value: 1). (b) Fernblock® supplementation reverts the decrease in viability associated with UVB exposure in keratinocytes, as assessed by cell counts. The effect of UVB exposure (grey bars) is normalized to the corresponding nonirradiated samples (black bars, expressed as 100% viability) for each Fernblock® treatment group. Data are derived from 3 independent biological replicates. n.s.: nonstatistically significant; $*$ and $^{\#}p \leq 0.05$. (c) Fernblock® induces the activity of a synthetic NRF2-dependent luciferase minigene reporter. Stable PC12 cells bearing a NQO1-driven minimal promoter were treated as indicated (vehicle: DMSO; time: 24 h). Data are normalized to control, which is expressed as 100% signal. $n = 3$. (d–h) mRNA expression levels ($^{-\Delta\Delta Ct}$ quantitation method) for indicated genes in human keratinocytes across indicated treatments were assessed by qRT-PCR using TaqMan technology. Data are normalized to the control (vehicle). $n = 3$. (i) mRNA expression levels for either IL6 (black bars) or IL8 (grey bars) across indicated treatment conditions in keratinocytes were assessed by qRT-PCR using TaqMan technology. $n = 3$. (j) Induction of keratinocyte melanization by the indicated treatments was assessed as detailed in Materials and Methods. Data are derived from absorbance across the visible spectrum and normalized to values from control samples. $n = 3$. $*p \leq 0.05$, $**p \leq 0.01$, $***p \leq 0.005$, and $****p \leq 0.0001$.

a moderate increase in NQO1 levels in the absence of $PM_{2.5}$ and significantly boosted their upregulation associated with $PM_{2.5}$ exposure, in accordance with the measurements recorded for NRF2 protein (Figures 4(c) and 4(d)). HO-1 protein levels exhibited an analogous response and Fernblock® significantly enhanced the upregulation associated with $PM_{2.5}$ exposure, as compared to the protective response observed in cells exposed to this particle pollution alone (Figures 5(a) and 5(b)).

4. Discussion

Air pollution is a major challenge to public health and well-being in modern societies, negatively impacting conditions such as cardiovascular disease, respiratory ailments and infections, and cancer. Thus, identifying compounds with protective properties against tissue damage due to this environmental source of xenotoxins is a priority for public health. An organ particularly exposed to damage from pollutants is the skin, and several cutaneous disorders are significantly influenced by environmental xenotoxins. Cellular mechanisms contrasting environmental pollutants include the AhR pathway, which positively regulates cyp450 detoxification systems and artemin [24]; the metal regulatory transcription factor-1 (MTF-1), which promotes the expression of antioxidant genes and metallothioneins in response to accumulation of heavy metals such as silver, cadmium, copper, or zinc [25]; and the conserved NRF2 pathway, which determines broad antioxidant and detoxifying transcriptional processes in response to different
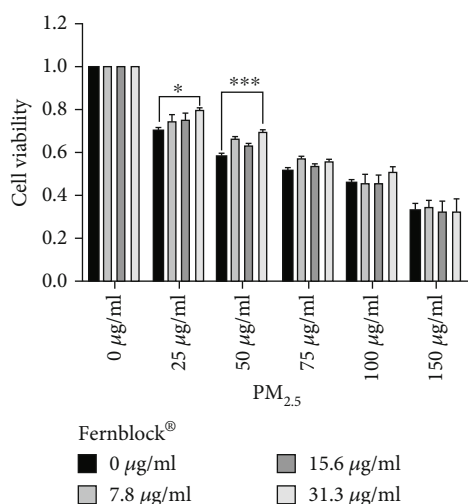
FIGURE 2: Fernblock® protects keratinocytes from $PM_{2.5}$-induced toxicity. MTT assay was performed on HaCaT samples across indicated treatments on $PM_{2.5}$, Fernblock®, or combinations of both compounds (see Materials and Methods). All data are expressed as normalized to untreated samples (leftmost bar group of graph). $n = 3$. $^*p \leq 0.05$ and $^{***}p \leq 0.005$.

forms of stress leading to accumulation of ROS and electrophilic stress [9–13]. As such, NRF2 activity has emerged as a particularly attractive target for therapeutic and antiaging skin treatment [11, 26].

Natural compounds able to modulate these protective endogenous pathways are a promising option to reduce the impact of environmental pollution on skin. Several such compounds have in fact been identified which promote the NFR2 cytoprotective activities, including sulforaphane (from cruciferous vegetables) [21], curcumin (from *Curcuma longa*) [27], cinnamaldehyde (from cinnamon) [28], or tanshinones (from *Salvia miltiorrhiza*) [29]. Here, we provide evidence that Fernblock®, a standardized aqueous extract from *Polypodium leucotomos* leaves with proven photoprotective properties *in vivo* and *in vitro* against radiation damage in skin [16–19, 30], also induces protective mechanisms in an experimental model of fine particle $PM_{2.5}$ air pollutants. Moreover, our studies provide novel evidence that the NRF2 transcriptional network is a relevant target upregulated by treatment with Fernblock® and demonstrate a close correlation between the upregulation of these antioxidant signalling pathways and the protective effect against damage from both UVB irradiation and fine particle pollutants. Due to their xenotoxic effect, $PM_{2.5}$ exposure markedly increased total NRF2 protein levels as a defense mechanism, suggesting acute robust activation to counteract oxidative damage (Figures 4(a) and 4(b)). Fernblock® supplementation preferentially increased nuclear pools of NRF2. These observations support a hypothesis whereby Fernblock® is able to increase basal NRF2 activity levels in the absence of xenotoxic agent and further enhance its activation induced against $PM_{2.5}$-induced oxidative stress, thus boosting the cell protection from damage. Several canonical routes downstream NRF2 (including autophagy and the direct NRF2 targets HO-1

and NQO1 which were demonstrated to be significantly impacted by Fernblock®) might play a role in the observed protection against $PM_{2.5}$ damage. Of note, our observations of net protein level upregulation across conditions for the NRF2 targets HO-1 and NQO1 (Figures 4 and 5), together with our data showing a lack of impact on cell proliferation/viability (Figure 1), support a scenario whereby Fernblock® does not provoke cell toxicity and potentially positively regulates NRF2 through other mechanisms (*see below*). The crosstalk between NRF2 with other pathways such as AhR or NF-κB-dependent inflammation networks involved in skin cell adaption to xenotoxins should also be taken into consideration [31, 32]. In addition to the cytoprotective routes driven by NRF2 in most cell types, an important factor to consider is the substantial impact NRF2 has on keratinocyte homeostasis through direct transcriptional control of different specialized structures, such as late cornified envelope 1 (LCE1) family members, keratins, and desmosomal components [33, 34].

Priming of autophagy, an important prosurvival and repairing mechanism [35], has also been demonstrated to be induced by treatment with Fernblock®. These studies thus also raise the important question as to how Fernblock® specifically interacts with cell metabolism, particularly interesting for its systemic (nutraceutical) applications. Modulation of key nodes of energy metabolism regulatory networks that also intersect with autophagy and ROS management, such as AMPK, is amenable though the use of well-established compounds such as metformin [36].

An important consideration that arises from these observations is the potential these mechanisms may have to slow skin aging. Loss of proteostasis and dysregulation of ROS levels and inflammation, decreased autophagy flux, and reduced NRF2 activity are all hallmarks of aging [37]. As stated above, NRF2 has also emerged as a relevant direct transcriptional regulator ensuring the expression of specialized keratinocyte components that decline with age, such as desmosomal proteins. Treatment with Fernblock® is effective for reducing radiation-induced cell senescence and age-associated damage in keratinocytes [17]. The present body of work further highlights the value of Fernblock® as an antiaging agent, whose beneficial effect might be the result of improved NRF2 signalling and autophagy. The potential of these mechanisms to attenuate accumulated oxidative stress and tissue damage is further exemplified by the reduction of UVB-induced melanogenesis, which is closely related to inflammation and oxidative stress in an evolutionarily conserved manner [38]. Adaptive pathways downstream NRF2, including Pi3/Akt signalling [39], autophagy itself [40, 41], and antioxidant effectors (potentially even by inhibiting the oxidative process of melanin biogenesis [42]), have been shown to contrast melanogenesis. Our observations support a model whereby Fernblock® reduces melanogenesis at least in part through upregulation of NRF2-dependent responses.

How does Fernblock® stimulate these prosurvival pathways? While other compounds currently being explored as "boosters" of NRF2 signalling, such as sulforaphane, exert their positive regulation of cytoprotection through canonical
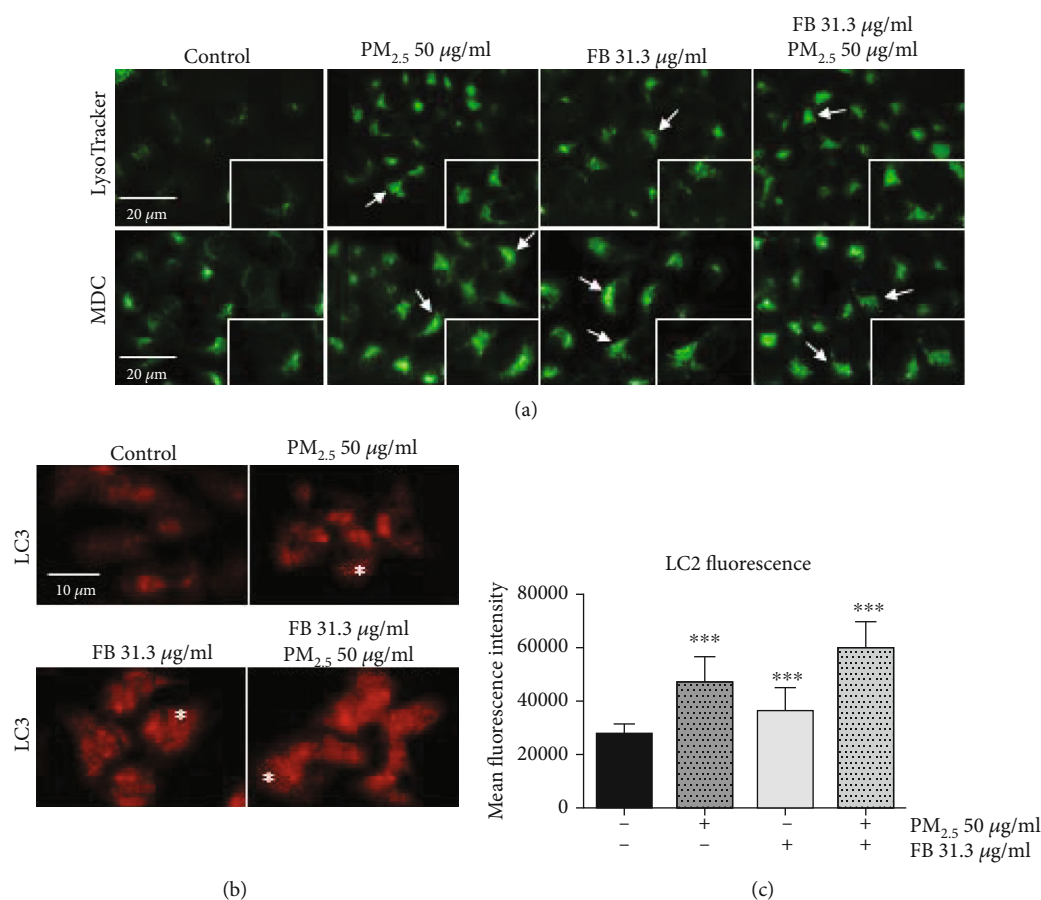
(a)

(b)

(c)

FIGURE 3: Fernblock® (FB) induces autophagolysosomal activity in keratinocytes *per se* and boosts autophagy flux in PM$_{2.5}$-treated cells. (a) Expansion of the lysosomal compartment (LysoTracker Green™, top panel row) and density of autophagolysosomal vacuoles (MDC, lower panel row) were acquired by immunofluorescence microscopy across indicated treatments in HaCaT cells. Scale bar for whole-field images (20 microns) and 3x enlarged insets are indicated. Cells with significant enlargement of their MDC-positive compartment are indicated with arrows (b, c) Density of LC3 punctate staining, as a proxy for autophagy flux activation, was assessed from immunofluorescence microscopy images on HaCaT cells treated as indicated (see Materials and Methods). Exemplary cells with increased punctate pattern staining are highlighted with asterisks in panels at (b). Data plotted in (c) were derived from 50 cells from 3 independent biological replicates. $^{***}p \leq 0.005$.

mechanisms [22], exact information regarding the molecular mechanisms by which Fernblock® modulates NRF2 and autophagy is lacking. A possible candidate mechanism could be the upregulation of sestrin family proteins, which have recently emerged as pivotal regulators upstream autophagy and ROS management in the cell [43]. A nonexclusive mechanism might be the modulation of cell metabolism and ROS production itself, currently not completely characterized for Fernblock®. It should be noted that autophagy is a relevant target of NRF2 itself: NRF2 drives the expression of essential autophagy regulators such as p62 and LAMP2A, and NRF2 deficiency reduces autophagy flux and favours the accumulation of proteotoxicity precursors [44, 45]. Our observations would agree with a speculative model whereby Fernblock® increases basal autophagy downstream enhanced NRF2 activity. Conversely, autophagy might also contribute to NRF2 activation through KEAP1 turnover, a mechanism likely underpinning the control of ROS through autophagy [46]. An intriguing additional potential mechanism both for Fernblock® antixenotoxic protection in general and for

NRF2 regulation in particular may be embodied by the proteostatic network of the Heat Shock Protein response, which suppresses NF-κB activity [47]. Because the identification of tools for promoting exogenous intervention of NRF2 signalling is an important objective across a broad range of fields in biomedicine, our findings highlight a potential use for Fernblock® as a natural compound able to upregulate this pathway, deserving of future research.

While the exact molecular mechanisms responsible for the loss of cell homeostasis upon exposure to PM$_{2.5}$, and their modulation upon treatment with Fernblock®, remain to be fully characterized, our observations support a general model whereby Fernblock® reduces xenotoxicity by priming prosurvival antistress pathways, such as the NRF2 pathway and autophagy, thus reducing the oxidative stress and cell damage provoked by harmful agents such as PM$_{2.5}$. Full characterization of the mechanisms modulated by Fernblock® may provide a framework for establishing personalized intervention and synergistic combinations that simultaneously boost these mechanisms as required.
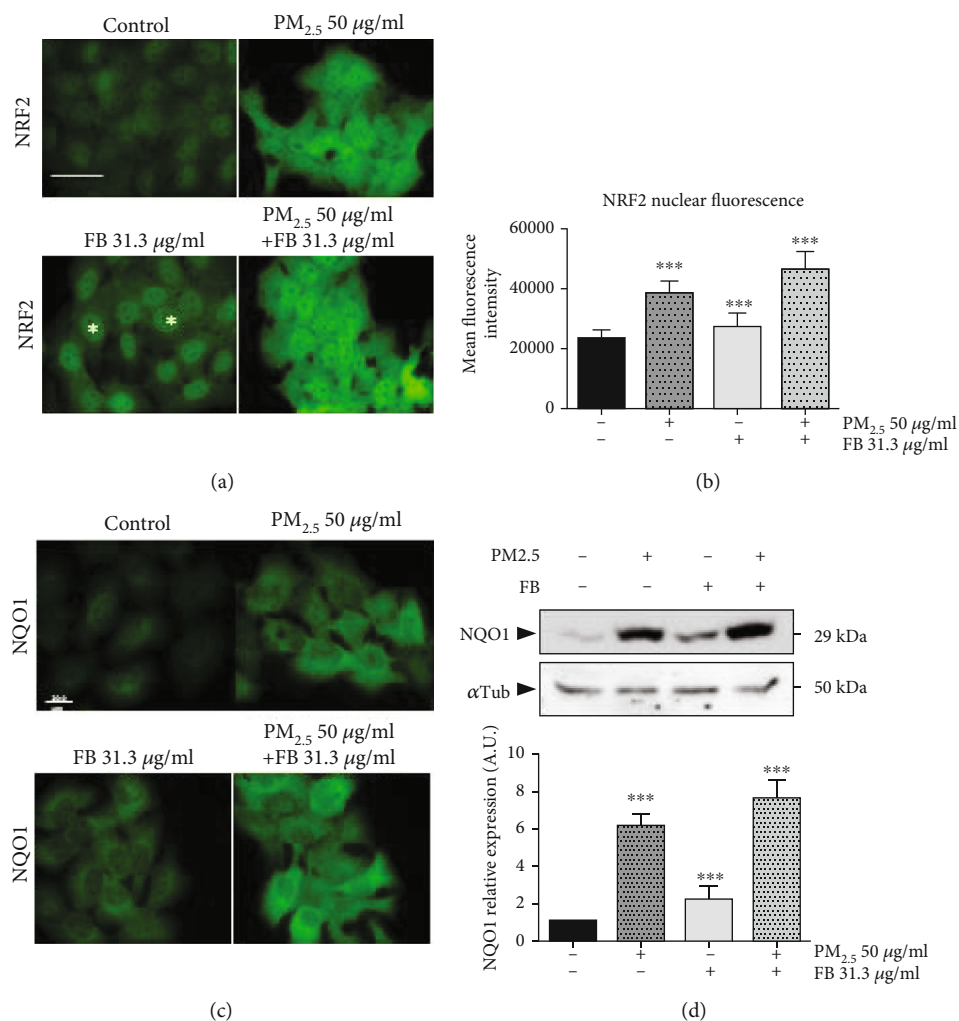
(a)

(b)

(c)

(d)

Figure 4: Fernblock® (FB) induces NRF2 activation and downstream transcription in keratinocytes. (a, b) NRF2 induction and activation was monitored in HaCaT cells by immunofluorescence microscopy across indicated treatment conditions. Scale bar (20 microns) is indicated. Exemplary cells with increased NRF2 staining specifically at the nuclear compartment are highlighted with asterisks in panel (a). Data plotted in (b) was derived from 50 cells from 3 independent biological replicates across conditions and expressed as normalized to untreated cells. (c, d) NQO1 induction downstream NRF2 was assessed in HaCaT cells by immunofluorescence microscopy (c) and immunoblotting (d, upper panel) across indicated conditions. (d, lower panel) Densitometric analysis of western blot data from 3 independent biological replicates is plotted as normalized to the signal observed in untreated cells. $^{***}p \leq 0.005$.
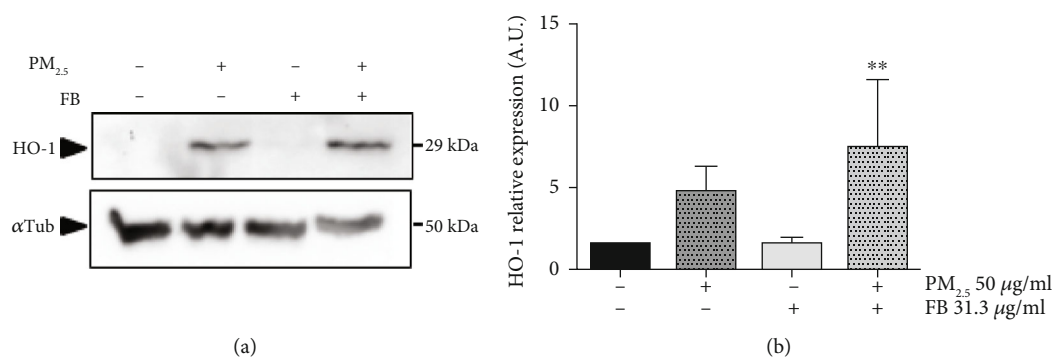

(a)

(b)

Figure 5: Fernblock® (FB) induces NRF2 activation and downstream transcription in keratinocytes. (a, b) HO-1 induction downstream NRF2 was assessed in HaCaT cells by immunoblotting (a, upper panel) across indicated conditions. (b) Densitometric analysis of western blot data from 3 independent biological replicates is plotted as normalized to the signal observed in untreated cells. $^{**}p \leq 0.01$.
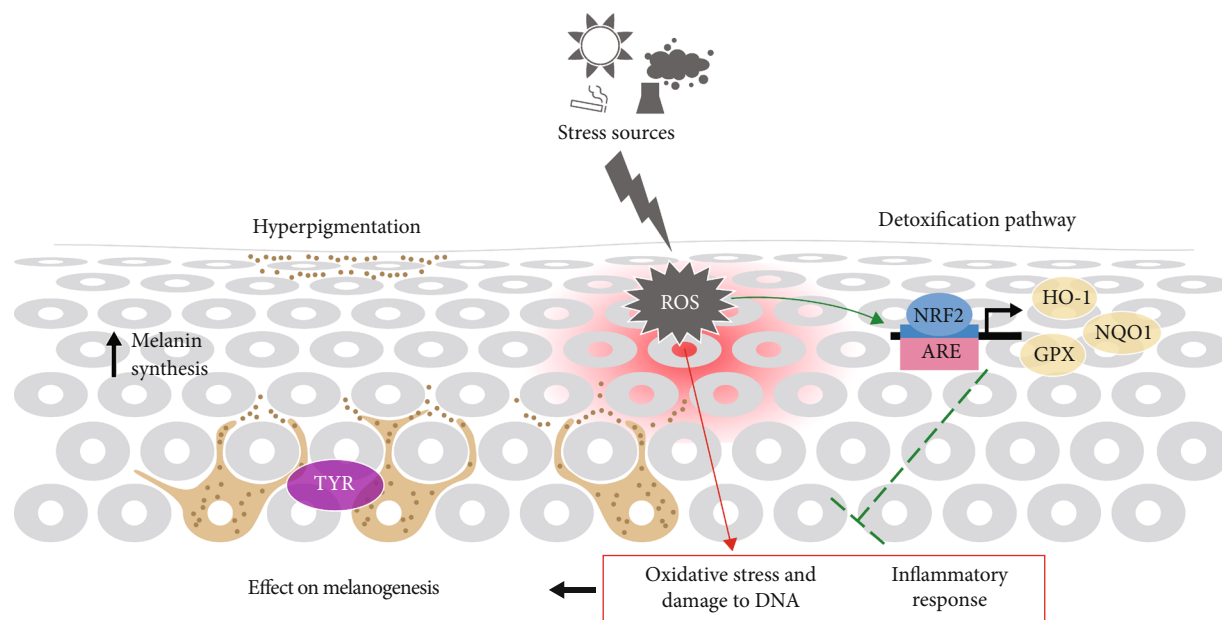
FIGURE 6: Scheme summarizing mechanisms identified in this study as potential sources of protection induced by Fernblock® against environmental damage of the skin.

5. Conclusions

Our results support NRF2 activation as a potential part of Fernblock®'s protective activity. Moreover, these studies have provided novel evidence that this protective activity is effective against not only oxidative stress derived from UVB radiation but also xenotoxic stress associated with exposure to fine particulate pollutants. Our observations strengthen the notion that Fernblock® can represent a functionally relevant and versatile compound effective against a wide range of environmental sources of tissue damage and aging and support its potential as a valuable tool (fully approved for human use) to elicit NRF2-dependent antistress responses across a wide range of conditions (graphical abstract, Figure 6).

Data Availability

All cell biology, biochemistry and microscopy data supporting the findings of this report are included in this article. Source raw data for all quantitations is fully available upon request.

Conflicts of Interest

S.G. has a consultant role for Cantabria Labs, and A. R.-L. belongs to the Medical Affairs Department at Cantabria Labs, which produced Fernblock®. Y.I. and Y.H. belong to the Rohto Basic Research Development Division, which distributed Fernblock®. The remaining authors declare no conflict of interest.

Authors' Contributions

Pablo Delgado-Wicke and Azahara Rodríguez-Luna contributed equally to this work.

Acknowledgments

Supplementary Materials

Figure S1: additional regional intensity analysis for NRF2 staining images from Figure 4(a) are shown. Data plotted are derived from the same image collections as in Figure 4(b). $^{***}p \leq 0.005$. (Supplementary Materials)

References

[1] World Health Organization, *Air Pollution And Health: Summary*, 2020, http://www9.who.int/airpollution/ambient/about/en/.

[2] P. Puri, S. K. Nandar, S. Kathuria, and V. Ramesh, "Effects of air pollution on the skin: a review," *Indian Journal of Dermatology, Venereology and Leprology*, vol. 83, no. 4, p. 415, 2017.

[3] M. J. Piao, M. J. Ahn, K. A. Kang et al., "Particulate matter 2.5 damages skin cells by inducing oxidative stress, subcellular organelle dysfunction, and apoptosis," *Archives of Toxicology*, vol. 92, no. 6, article 2197, pp. 2077–2091, 2018.

[4] Q. Li, Y. Yang, R. Chen et al., "Ambient air pollution, meteorological factors and outpatient visits for eczema in Shanghai, China: a time-series analysis," *International Journal of Environmental Research and Public Health*, vol. 13, no. 11, p. 1106, 2016.

[5] M. Kim, L. Y. Li, and J. R. Grace, "Predictability of physico-chemical properties of polychlorinated dibenzo-p-dioxins (PCDDs) based on single-molecular descriptor models," *Environmental Pollution*, vol. 213, pp. 99–111, 2016.

[6] C. Juliano and G. Magrini, "Cosmetic ingredients as emerging pollutants of environmental and health concern. A mini-review," *Cosmetics*, vol. 4, no. 2, p. 11, 2017.

[7] A. Zamarrón, E. Morel, S. Lucena et al., "Extract of *Deschampsia antarctica* (EDA) prevents dermal cell damage induced by UV radiation and 2,3,7,8-tetrachlorodibenzo-p-dioxin," *International Journal of Molecular Sciences*, vol. 20, no. 6, article 1356, 2019.

[8] L. Marrot, "Pollution and sun exposure: a deleterious synergy. Mechanisms and opportunities for skin protection," *Current Medicinal Chemistry*, vol. 25, no. 40, pp. 5469–5486, 2018.

[9] P. Moi, K. Chan, I. Asunis, A. Cao, and Y. W. Kan, "Isolation of NF-E2-related factor 2 (Nrf2), a NF-E2-like basic leucine zipper transcriptional activator that binds to the tandem NF-E2/AP1 repeat of the beta-globin locus control region," *Proceedings of the National Academy of Sciences of the United States of America*, vol. 91, no. 21, pp. 9926–9930, 1994.

[10] P. Shaw and A. Chattopadhyay, "Nrf2–ARE signaling in cellular protection: mechanism of action and the regulatory mechanisms," *Journal of Cellular Physiology*, vol. 235, no. 4, pp. 3119–3130, 2019.

[11] M. C. Lu, J. A. Ji, Z. Y. Jiang, and Q. D. You, "The Keap1–Nrf2–ARE pathway as a potential preventive and therapeutic target: an update," *Medicinal Research Reviews*, vol. 36, no. 5, pp. 924–963, 2016.

[12] X. Deng, W. Rui, F. Zhang, and W. Ding, "PM2.5 induces Nrf2-mediated defense mechanisms against oxidative stress by activating PIK3/AKT signaling pathway in human lung alveolar epithelial A549 cells," *Cell Biology and Toxicology*, vol. 29, no. 3, pp. 143–157, 2013.

[13] H. Zhang, H. Liu, K. J. Davies et al., "Nrf2-regulated phase II enzymes are induced by chronic ambient nanoparticle exposure in young mice with age-related impairments," *Free Radical Biology and Medicine*, vol. 52, no. 9, pp. 2038–2046, 2012.

[14] L. Gombau, F. García, A. Lahoz et al., "Polypodium leucotomos extract: antioxidant activity and disposition," *Toxicology in Vitro*, vol. 20, no. 4, pp. 464–471, 2006.

[15] S. Z. Choudhry, N. Bhatia, R. Ceilley et al., "Role of oral *Polypodium leucotomos* extract in dermatologic diseases: a review of the literature," *Journal of Drugs in Dermatology*, vol. 13, no. 2, pp. 148–153, 2014.

[16] S. Gonzalez, Y. Gilaberte, N. Philips, and A. Juarranz, "Fernblock, a nutriceutical with photoprotective properties and potential preventive agent for skin photoaging and photoinduced skin cancers," *International Journal of Molecular Sciences*, vol. 12, no. 12, pp. 8466–8475, 2011.

[17] A. Zamarrón, S. Lorrio, S. González, and Á. Juarranz, "Fernblock prevents dermal cell damage induced by visible and infrared a radiation," *International Journal of Molecular Sciences*, vol. 19, no. 8, article 2250, 2018.

[18] C. Parrado, M. Mascaraque, Y. Gilaberte, A. Juarranz, and S. Gonzalez, "Fernblock (Polypodium leucotomos extract): molecular mechanisms and pleiotropic effects in light-related skin conditions, photoaging and skin cancers, a review," *International Journal of Molecular Sciences*, vol. 17, no. 7, article 1026, 2016.

[19] B. Berman, C. Ellis, and C. Elmets, "*Polypodium leucotomos* - an overview of basic investigative findings," *Journal of Drugs in Dermatology*, vol. 15, no. 2, pp. 224–228, 2016.

[20] B. Bao, M. Q. Zhang, Z. Y. Chen et al., "Sulforaphane prevents PC12 cells from oxidative damage via the Nrf2 pathway," *Molecular Medicine Reports*, vol. 19, no. 6, pp. 4890–4896, 2019.

[21] Y. Morimitsu, Y. Nakagawa, K. Hayashi et al., "A sulforaphane analogue that potently activates the Nrf2-dependent detoxification pathway," *Journal of Biological Chemistry*, vol. 277, no. 5, pp. 3456–3463, 2002.

[22] X. Su, X. Jiang, L. Meng, X. Dong, Y. Shen, and Y. Xin, "Anticancer activity of sulforaphane: the epigenetic mechanisms and the Nrf2 signaling pathway," *Oxidative Medicine and Cellular Longevity*, vol. 2018, Article ID 5438179, 10 pages, 2018.

[23] N. D. Magnani, X. M. Muresan, G. Belmonte et al., "Skin damage mechanisms related to airborne particulate matter exposure," *Toxicological Sciences*, vol. 149, no. 1, pp. 227–236, 2016.

[24] T. Hidaka, E. Ogawa, E. H. Kobayashi et al., "The aryl hydrocarbon receptor AhR links atopic dermatitis and air pollution via induction of the neurotrophic factor artemin," *Nature Immunology*, vol. 18, no. 1, pp. 64–73, 2017.

[25] W. Wu, P. A. Bromberg, and J. M. Samet, "Zinc ions as effectors of environmental oxidative lung injury," *Free Radical Biology and Medicine*, vol. 65, pp. 57–69, 2013.

[26] M. R. de la Vega, A. Krajisnik, D. Zhang, and G. Wondrak, "Targeting NRF2 for improved skin barrier function and photoprotection: focus on the achiote-derived apocarotenoid bixin," *Nutrients*, vol. 9, no. 12, article 1371, 2017.

[27] X. Lin, D. Bai, Z. Wei et al., "Curcumin attenuates oxidative stress in RAW264.7 cells by increasing the activity of antioxidant enzymes and activating the Nrf2-Keap1 pathway," *PLoS One*, vol. 14, no. 5, article e0216711, 2019.

[28] T.-C. Huang, Y.-L. Chung, M.-L. Wu, and S.-M. Chuang, "Cinnamaldehyde enhances Nrf2 nuclear translocation to upregulate phase II detoxifying enzyme expression in HepG2 cells," *Journal of Agricultural and Food Chemistry*, vol. 59, no. 9, pp. 5164–5171, 2011.

[29] S. Tao, Y. Zheng, A. Lau et al., "Tanshinone I activates the Nrf2-dependent antioxidant response and protects against As(III)-induced lung inflammation *in vitro* and *in vivo*," *Antioxidants & Redox Signaling*, vol. 19, no. 14, pp. 1647–1661, 2013.

[30] P. Torricelli, M. Fini, P. A. Fanti, E. Dika, and M. Milani, "Protective effects of Polypodium leucotomosextract against UVB-induced damage in a model of reconstructed human epidermis," *Photodermatology, Photoimmunology & Photomedicine*, vol. 33, no. 3, pp. 156–163, 2017.

[31] S. Shin, N. Wakabayashi, V. Misra et al., "NRF2 modulates aryl hydrocarbon receptor signaling: influence on adipogenesis," *Molecular and Cellular Biology*, vol. 27, no. 20, pp. 7188–7197, 2007.

[32] J. D. Wardyn, A. H. Ponsford, and C. M. Sanderson, "Dissecting molecular cross-talk between Nrf2 and NF-κB response pathways," *Biochemical Society Transactions*, vol. 43, no. 4, pp. 621–626, 2015.

[33] M. Schäfer, H. Farwanah, A. H. Willrodt et al., "Nrf2 links epidermal barrier function with antioxidant defense," *EMBO Molecular Medicine*, vol. 4, no. 5, pp. 364–379, 2012.

[34] A. J. Huebner, D. Dai, M. Morasso et al., "Amniotic fluid activates the nrf2/keap1 pathway to repair an epidermal barrier defect in utero," *Developmental Cell*, vol. 23, no. 6, pp. 1238–1246, 2012.

[35] V. M. Hubbard, R. Valdor, F. Macian, and A. M. Cuervo, "Selective autophagy in the maintenance of cellular homeostasis in aging organisms," *Biogerontology*, vol. 13, no. 1, pp. 21–35, 2012.

[36] M. Foretz and B. Viollet, "Therapy: metformin takes a new route to clinical efficacy," *Nature Reviews Endocrinology*, vol. 11, no. 7, pp. 390–392, 2015.

[37] C. López-Otín, M. A. Blasco, L. Partridge, M. Serrano, and G. Kroemer, "The hallmarks of aging," *Cell*, vol. 153, no. 6, pp. 1194–1217, 2013.

[38] H. Bilandžija, M. Laslo, M. L. Porter, and D. W. Fong, "Melanization in response to wounding is ancestral in arthropods and conserved in albino cave species," *Scientific Reports*, vol. 7, no. 1, article 17148, 2017.

[39] J.-M. Shin, M. Y. Kim, K. C. Sohn et al., "Nrf2 negatively regulates melanogenesis by modulating PI3K/Akt signaling," *PLoS One*, vol. 9, no. 4, article e96035, 2014.

[40] E. S. Kim, H. Chang, H. Choi et al., "Autophagy induced by resveratrol suppresses α-MSH-induced melanogenesis," *Experimental Dermatology*, vol. 23, no. 3, pp. 204–206, 2014.

[41] Y. Yang, G. B. Jang, X. Yang et al., "Central role of autophagic UVRAG in melanogenesis and the suntan response," *Proceedings of the National Academy of Sciences*, vol. 115, no. 33, pp. E7728–E7737, 2018.

[42] A. Chaiprasongsuk, T. Onkoksoong, T. Pluemsamran, S. Limsaengurai, and U. Panich, "Photoprotection by dietary phenolics against melanogenesis induced by UVA through Nrf2-dependent antioxidant responses," *Redox Biology*, vol. 8, pp. 79–90, 2016.

[43] M. Cordani, M. Sánchez-Álvarez, R. Strippoli, A. V. Bazhin, and M. Donadelli, "Sestrins at the interface of ROS control and autophagy regulation in health and disease," *Oxidative Medicine and Cellular Longevity*, vol. 2019, Article ID 1283075, 11 pages, 2019.

[44] M. Pajares, N. Jiménez-Moreno, Á. J. García-Yagüe et al., "Transcription factor NFE2L2/NRF2 is a regulator of macroautophagy genes," *Autophagy*, vol. 12, no. 10, pp. 1902–1916, 2016.

[45] M. Pajares, A. I. Rojo, E. Arias, A. Díaz-Carretero, A. M. Cuervo, and A. Cuadrado, "Transcription factor NFE2L2/NRF2 modulates chaperone-mediated autophagy through the regulation of LAMP2A," *Autophagy*, vol. 14, no. 8, pp. 1310–1322, 2018.

[46] S. Pankiv, T. H. Clausen, T. Lamark et al., "p62/SQSTM1 binds directly to Atg8/LC3 to facilitate degradation of ubiquitinated protein aggregates by autophagy," *Journal of Biological Chemistry*, vol. 282, no. 33, pp. 24131–24145, 2007.

[47] J. P. Stice and A. A. Knowlton, "Estrogen, NFκB, and the heat shock response," *Molecular Medicine*, vol. 14, no. 7-8, pp. 517–527, 2008.